In: Advances in Chemistry Research. Volume 11
Editor: James C. Taylor, pp. 1-16
ISBN 978-1-61324-815-7

Chapter 11

PROTECTION OF BRONZE BY NEW NON-TOXIC CORROSION INHIBITORS FROM THE INFLUENCE OF ARTIFICIAL ACID RAIN

K. Marušić and H. Otmačić Ćurković
Faculty of Chemical Engineering and Technology, University of Zagreb, Croatia

ABSTRACT

Bronze is a metal commonly used for sculptures and building structures. These objects are often covered with patina, a layer of corrosion products, which confers their aesthetic and also protects the substrate bronze. Due to the increasing atmospheric pollution these layers, as well as the supstrate bronze, are often dissolving when exposed in urban environment.

This work proposes the use of two innoxious imidazole compounds as corrosion inhibitors: 4-methy1-1-*p*-tolylimidazole (TMI) and 1-*H* benzimidazole (BZI) on the Cu-6Sn (wt-%) bronze, in a solution simulating acid rain in urban environments. The results of the electrochemical investigations have shown that both TMI, as well as BZI protect this alloy.

On the Cu-6Sn bronze patina was formed by a new electrochemical method which simulates patina formed spontaneously during long term exposure to urban environments. As corrosion inhibitors both TMI and BZI were applied on patina in the solution simulating acid rain. The results have shown that they both improve greatly the stability of patina. The results confirmed that both TMI and BZI can be used for protection of bronze, as well as its patina exposed to urban environments.

1. INTRODUCTION

Corrosion is a damaging process of a material, especially metal, which results from its reaction with the environment it is exposed to. Many structural alloys corrode merely from exposure to moisture in air, but this process can be strongly affected by presence of certain substances, such as CO_2, SO_2, NO_x, O_2, seawater, etc.

Bronze is one of the oldest alloys which has been used for a very long time for sculptures and for building structures such as roofs and gutters. Many copper roofs have lasted for centuries on castles, churches and other monumental buildings. During the period when these artifacts have been exposed to its environment a layer of corrosion products called patina will be formed spontaneously.

Because of its aesthetic aspect and also due to the subjective association to antique artifacts, patinas are often deliberately added by artists and metalworkers. Scientists are interested in the mechanism of patina formation and the protection of cultural heritage for future generations, thus they have recourse to synthetic patina. Patinas may be used to 'antique' objects, as a part of the design or decoration of art and furniture during restorations.

In other terms, it is possible to distinguish two kinds of patina:

- The first one is *natural patina* formed spontaneously during long time exposure of a metal to its environment. The structure and composition of patina and bronzes are specific to each case due to the metallurgy of bronze itself and also to the environment surrounding the bronze artifact.
- The second type is *synthetic* or *artificial patina* with a defined chemical composition that can be formed in laboratory or foundry workshop allowing appropriate accelerated surface treatment of bronze. [1, 2]

Colored natural patinas form spontaneously on copper alloys by very slow corrosion processes. They are a result of a chemical interaction with the main composition of air, humidity, oxygen and carbonate, and also with trace amounts of pollutants in the atmosphere, particularly, sulphates, and chlorides, although other elements such as NO_2, O_3, H_2S play a role. [3] The color depends on the corrosion products formed, which depend partly on the alloy and partly on the environment. Particularly, copper or bronzes exposed to urban atmospheres for many decades exhibit a greenish patina, because of copper carbonate or sulphate crystals, containing several constituents that had been largely studied. [1, 3-15]

As for artificial or synthetic patinas, hundreds of recipes for patina formation are known. [16]. There are two kinds of patina synthesis: chemical synthesis, mostly used, and electrochemical synthesis used nowadays only for scientific purpose, since according to the “Conservation ethics” investigations should not be performed on cultural monuments. The patina electrochemically formed can be synthesized under current regulation. [2, 17, 18] However, this method produces a patina which does not cover uniformly the surface of bronze and goes deep in the core of the metal. For this reason a new method of electrochemical synthesis under potential regulation was developed. [18-20] Patina obtained by this method mimics much better naturally formed patina in an urban atmosphere.

Patina is composed of a variety of fine crystalline particles covering copper or bronze surface. Some of them adhere well to the surface, the others not. Each particle, however, can be identified as its homologous well defined mineral of a larger crystal.

A basic green coloration is given by emerald / dark-green malachite, basic copper(II) carbonate, $CuCO_3 \cdot Cu(OH)_2$, whilst, less commonly in very slightly humid environments, a blue color develops from another basic copper(II) carbonate, azurite, $2CuCO_3 \cdot Cu(OH)_2$. Carbonate patinas form in clean atmospheres. On some high-tin contained bronzes, white to grey turquoise patinas called ‘water’ patinas are found, and consist mainly of tin oxide, SnO_2.

The hue of a patina can be reddened by an underlying layer of copper(I) oxide, cuprite, Cu_2O. [3, 19, 21]

In sulphate environments (urban atmosphere), the initial corrosion product is cuprite, Cu_2O, with posnjakite, $Cu_4(SO_4)(OH)_6 \cdot H_2O$. [22] Posnjakite is either 'washed away' or converted to brochantite, $CuSO_4 \cdot 3Cu(OH)_2$, after longer exposure. The amount of brochantite increases with exposure time and forms a green-blue patina layer. [23] Even before industrialization, there was enough hydrogen sulphide and sulphur dioxide in air to induce its formation. [21]

In chloride containing environments (marine), the initial phase of corrosion product to be formed is cuprite, with paratacamite, $Cu_2Cl(OH)_3$, an isomorphic compound of atacamite, which appears as a secondary phase growing on the cuprite. Atacamite also appears after longer exposures. Both atacamite and paratacamite present a green-blue colouring, characteristic for the copper patinas formed in marine atmospheres. [5] The phases commonly found on copper specimens weathered in the atmosphere are summarized below: [24]

- *Cuprite* [Cu_2O]: Purple red. It is insoluble in water and slightly soluble in acid.
- *Brochantite* [$Cu_4(SO_4) \cdot Cu(OH)_2$]: Green-bleu. It is nearly always the most common component of the green patina formed on copper after long atmospheric exposures.
- *Antlerite* [$Cu_3(SO_4)(OH)_4$]: Deep green. This crystal form may be found in more acidic conditions than brochantite. [3] There is some evidence that antlerite may form at earlier stages of the patination process than brochantite. It is suggested that acid rain is converting brochantite to less protective antlerite, which is more susceptible to erosion.
- *Posnjakite* [$Cu_4(SO_4)(OH)_6 \cdot H_2O$]: Blue to dark blue. It is a precursor of brochantite and has a similar structure (hydrated form of brochantite).
- *Atacamite* [$Cu_2Cl(OH)_3$]: Green to yellow-green. It is soluble in weak acid. It was found to be as or more abundant than brochantite in patinas formed near seaside due to the influence of sea-salt aerosols. It is not found on specimens exposed for short periods.
- *Paratacamite* [$Cu_2Cl(OH)_3$]: Dark green to greenish black. Its presence is temporary and it eventually converts to atacamite. It is not found in patinas corresponding to long exposures.
- *Malachite* [$Cu_2(CO_3) \cdot Cu(OH)_2$]: Green to dark green. Atmospheric conditions do not favour the formation of this type of patina, but this basic carbonate is sometimes unexpectedly found in practice.
- *Azurite* [$2CuCO_3 \cdot Cu(OH)_2$]: Azure blue to blue. Azurite is unstable in open air, when compared with malachite, and therefore is often pseudomorphically replaced by it.
- *Gerhardtite* [$Cu_2NO_3(OH)_3$]: Green – dark green. It is also found in some locations.

Because of the markedly increasing air pollution and acid rain bronze and its patina exposed in urban environment are dissolving. Thus, additional protection is needed.

One of the most employed methods to mitigate corrosion is the use of inhibitors. Inhibitors are substances which, when added in small amounts to an aggressive media, reduce markedly the corrosion rate. In terms of corrosion, inhibitors occupy a special place because of their specific protection and widespread application. Most inhibitor applications are in

aqueous medium, partially water systems and protection from atmospheric corrosion. When selecting inhibitors, it should be taken into account what metal is to be protected, the environment to which the metal is exposed, the conditions in which the metal is submitted, and also their efficiency, availability, cost-effectiveness and importantly toxicity.

Until recently very efficient, but toxic, inhibitors have been used, e.g. chromates, sodium-nitrite, benzotriazol etc. Nowadays, many regulations and recommendations forbid or restrict the use of these inhibitors, so new non-toxic inhibitors are being developed, e.g. inhibitors of plant origin (green inhibitors), as well as synthetic non-toxic and self-degradable compounds. Imidazole derivatives are corrosion inhibitors, which satisfy these requirements.

Present studies were performed on Cu-6Sn binary bronze with and without artificial patina electrochemically formed. The aim of this work is to investigate the possibility of protecting bronze and its patina by new non-toxic imidazole derivatives as corrosion inhibitors.

2. EXPERIMENTAL

Investigations were performed on the Cu–6Sn (wt%) bronze. The composition of this alloy, determined according to DIN 17660 is given in Table 1.

Table 1. Elemental composition of the Cu–6Sn bronze.

	Sn	Pb	Zn	Fe	P	Cu
wt-%	6.10	0.01	0.10	0.02	0.11	93.66
at-%	3.36	0.01	0.10	0.02	0.23	96.28

Percentage normalized with analysed elements.

2.1. Electrodes

Bands of 10mm×10mm were cut out of 0.5mm thick rolled Cu–6Sn bronze sheets and connected by an electrical wire on the back side. To avoid the electrolyte infiltration they were covered with cataphoretic paint (PGGW975 + G323) and embedded into epoxy resin.

2.2. Patina formation

The bronze electrodes were polished and chemically degreased with ethanol. After that, six electrodes were connected in parallel (Fig. 1). They were dipped in an aerated solution composed of 0.2 $g \cdot L^{-1}$ Na_2SO_4 +0.2 $g \cdot L^{-1}$ $NaHCO_3$ at 30 °C. As the counter electrode a nickel wire was used, and the reference electrode a saturated calomel electrode. After a stable open circuit potential (OCP) was reached, which was usually about −0.05V versus SCE, patina was synthesized under potential control:

1. At −0.20V vs. OCP during 60 s,
2. at +0.14V vs. OCP during the next 48 h,

3. at +0.12V vs. OCP during another 48 h.

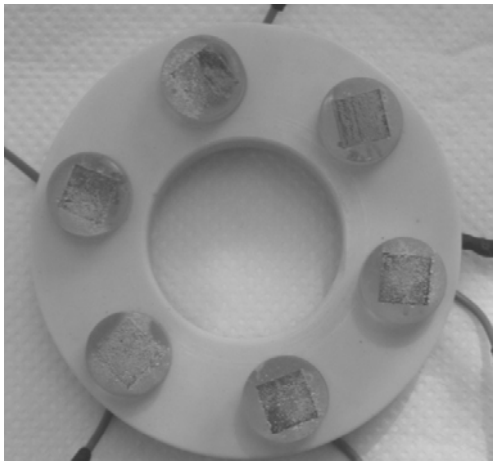

Figure 1. Parallel connection of six electrodes for the electrochemical patination.

2.3. Experimental investigations

The structure of artificial patina was examined with scanning electron microscopy (SEM; Leica Stereoscan 440 controlled by LEO software) and X-ray elemental energy dispersion spectroscopy (EDS analyses; Princeton Gamma-Tech, model Spirit) at 20 keV. Standard used for quantitative micro-analyses of oxygen was MgO while carbon and nitrogen were not taken into account for the quantitative analysis.

Measurements were performed using EG&G potentiostat/galvanostat Model 263A and frequency response detector 1025 monitored with PowerSINE software for EIS measurements.

2.4. Corrosion test solution

The corrosion test solution was 0.2 g L^{-1} Na_2SO_4 +0.2 g L^{-1} $NaHCO_3$ acidified to pH 5 by addition of dilute sulphuric acid at room temperature. This solution constitutes markedly simplified artificial acid rain in urban atmosphere. The presence of sulphate represents the pollution by sulphur dioxide frequently induced by petroleum in nowadays, and coal in ancient time. The presence of carbonate ions is due to the natural composition of air, i.e. 0.033 %. The absence of chloride in this test solution is representative of urban areas far from seaside.

The tested corrosion inhibitors were 4-methyl-1-*p*-tolyl imidazole (TMI) and 1-*H* benzimidazole (BZI), whose molecular structures are shown in Fig. 2. These compounds were dissolved in the test solution in different concentrations.

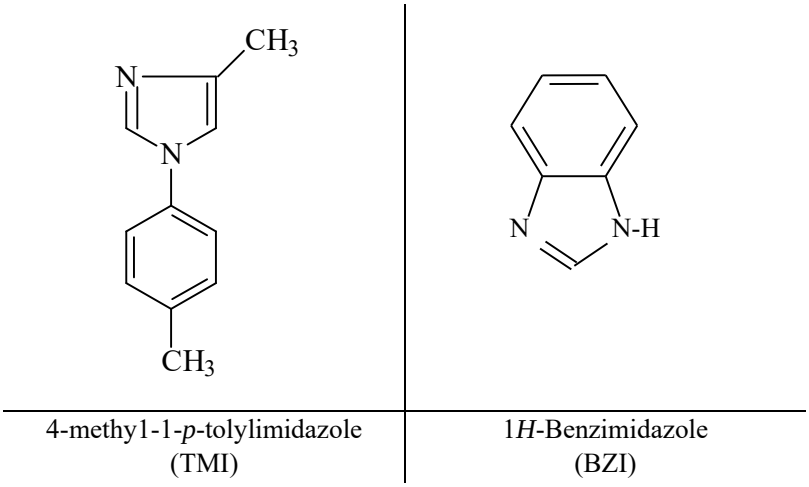

Figure 2. Molecular structure of the investigated imidazoles: TMI and BZI.

Polarization measurements were carried out in a conventional three-electrode cell (~ 100 mL volume). A saturated calomel electrode (SCE) was used as the reference and Pt plate as the counter electrode. All potentials are reported vs. SCE.

Electrochemical measurements were conducted after one hour immersion in the test solution with or without the inhibitor to avoid too important change of the open circuit potential during the collection of polarization or impedance data. The polarization curves were then plotted from the most negative potential about -0.15 V from the open circuit potential, towards the more positive direction up to about 0.15 V for the Tafel extrapolation method and from –0.02 to 0.02 V for the polarization resistance method, at the potential scan rate of 0.166 $mV \cdot s^{-1}$.

The data used for the Tafel extrapolation or the polarization resistance measurements were collected using the EG&G potentiostat / galvanostat Model 263A. For impedance measurements, frequency response detector 1025 was coupled to the above device. Experiments were monitored with PowerSine® software.

3. RESULTS

3.1. Bare bronze

The electrochemical investigations on bare bronze were performed in a specific order. After the electrodes were dipped in the test solution for one hour the polarization resistance method was performed. Afterwards the Tafel extrapolation method was applied. Since the polarization resistance method is performed in a narrow potential range (±20 mV), unlike the Tafel extrapolation method (±150 mV), the perturbing signal is much smaller and thus this method modifies the surface state of bronze to a less extent. This is the reason why the Tafel extrapolation method can be performed on the same specimen afterwards.

3.1.1. 4-methy1-1-*p*-tolylimidazole (TMI)

Results obtained by the anodic and cathodic polarization of bronze in wide potential range are shown in Fig. 3. They show that with addition of inhibitor, cathodic branches shift towards smaller currents up to the concentration of 5 mmol·dm^{-3}. Beyond this threshold concentration, the cathodic current increases. In contrast, the anodic branches shift towards the higher current direction up to 5 mmol·dm^{-3}, after which it no longer increases. As a whole, the open circuit potential displaces towards the more cathodic direction and also the corrosion current densities decrease up to 5 mmol·dm^{-3}. Consequently, TMI is a cathodic corrosion inhibitor.

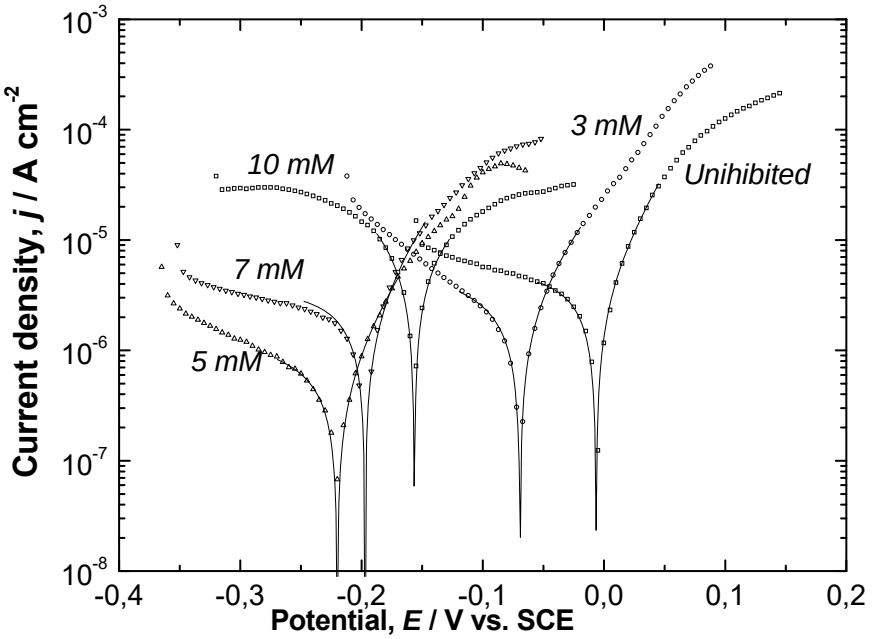

Figure 3. Wide potential range polarization curves of bare bronze with different TMI concentrations.

The linear Tafel segments of the cathodic curves and the calculated anodic Tafel lines were extrapolated to the corrosion potential to obtain the corrosion current densities (j_{corr}) and corrosion potential. The inhibition efficiency, z (%), was evaluated from the measured j_{corr} values using the relationship:

$$z(\%) = \frac{j_{corr,0} - j_{corr}}{j_{corr,0}} \times 100 \quad (1)$$

where $j_{corr,0}$ and j_{corr} are the corrosion current densities for uninhibited and inhibited solutions, respectively. The corrosion parameters are displayed in Table 2. The inhibitive efficiency is maximal at the concentration 5 mmol·dm^{-3} and is 84 %. At the concentration 10

mmol·dm^{-3}, the inhibitive efficiency is negative corresponding to the acceleration of the corrosion rate compared with the absence of TMI.

Table 2. Corrosion parameters of bare bronze with different TMI concentrations, determined by the Tafel extrapolation method.

c, mmol·dm^{-3}	/	1	3	5	7	10
E_{corr}, mV	-6.40	-78.1	-69.1	-220	-197	-157
b_a, mV·dec^{-1}	54.1	141	70.2	56.7	55.0	134
- b_c, mV·dec^{-1}	736	155	405	344	401	122
j_{corr}, µA·cm^{-2}	4.01	3.04	2.99	0.656	2.00	6.61
z, %	/	24.1	25.4	83.6	50.1	-64.5

Fig. 4 shows results obtained by the polarization of the bronze electrode in a narrow potential range. This figure illustrates that in presence of the inhibitor the slope of the polarization curve decreases corresponding to an increase of the polarization resistance.

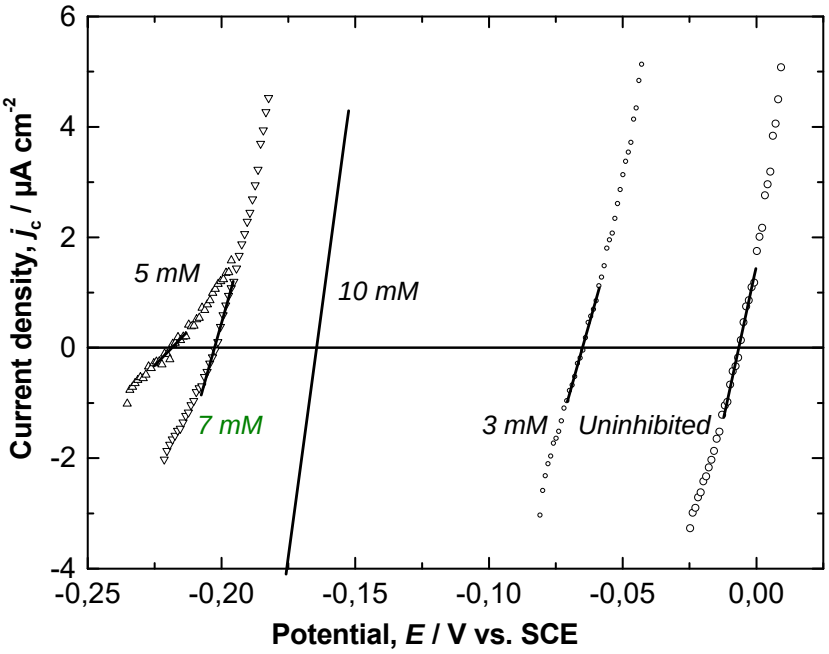

Figure 4. Narrow range polarization curves of bare bronze with different TMI concentrations.

The corrosion current density (I_{corr}) is calculated in this method from the polarization resistance (R_p) using the Stern-Geary equation, which is expressed as:

$$j_{corr} = \frac{B}{R_p} \tag{2}$$

where B is a constant with a voltage unit and R_p is the polarization resistance at the potential corresponding to a unit surface area of reinforcement. B is determined by the cathodic and anodic Tafel slopes $|b_c|$ and $|b_a|$:

$$B = \frac{|b_a \cdot b_c|}{|b_a| + |b_c|} \tag{3}$$

Corrosion parameters of the bronze electrode extracted from the polarization curves in a narrow potential range (Fig. 4) are shown in Table 3.

The corrosion current density calculated from the Stern – Geary relationship is in agreement with the Tafel extrapolation method. It decreases in presence of the inhibitor, and exhibits the smallest value at the inhibitor concentration 5 mmol·dm^{-3}. It can also be seen that the polarization resistance increases in presence of the inhibitor and is the highest at the concentration 5 mmol·dm^{-3}. At this concentration the inhibitive efficiency is 83 %. An excess of TMI however accelerates the corrosion rate, and at the concentration 10 mmol·dm^{-3} z is negative. This increase is essentially due to the increase of the cathodic current. One of the possibilities of this side-effect will be the reduction of TMI molecules rather than desorption of TMI from the bronze surface since the anodic current densities remain stable.

Table 3. Corrosion parameters of bare bronze in Na_2SO_4 / $NaHCO_3$ at pH 5 with different TMI concentrations, determined by polarization resistance method.

c, mmol·dm^{-3}	/	**1**	**3**	**5**	**7**	**10**
E_{corr}, mV	-7.02	-81.1	-64.9	-219	-203	-165
B, mV	21.9	31.6	26.0	21.1	21.0	28.2
R_p, kΩ·cm^2	4.50	8.09	7.38	25.1	7.60	3.02
j_{corr}, μA·cm^{-2}	4.87	3.91	3.51	0.84	2.76	9.44
Z, %	/	19.7	27.9	82.8	43.3	-93.8

3.1.2. 1-*H* benzimidazole

Results obtained by the anodic and cathodic polarization of the bronze electrode in wide potential range (Fig. 5) show that with addition of inhibitor both anodic and cathodic curves move towards smaller current densities indicating a mixed inhibitor property of BZI. It can be remarked also that the inhibitive effect on the cathodic process seems to no longer improve above 0.5 mmol·dm^{-3}. As for the anodic process, the current density continues, though moderately, to decrease. As a whole, the addition of inhibitor does not modify significantly the corrosion potential. Corrosion parameters evaluated from these curves are presented in Table 4.

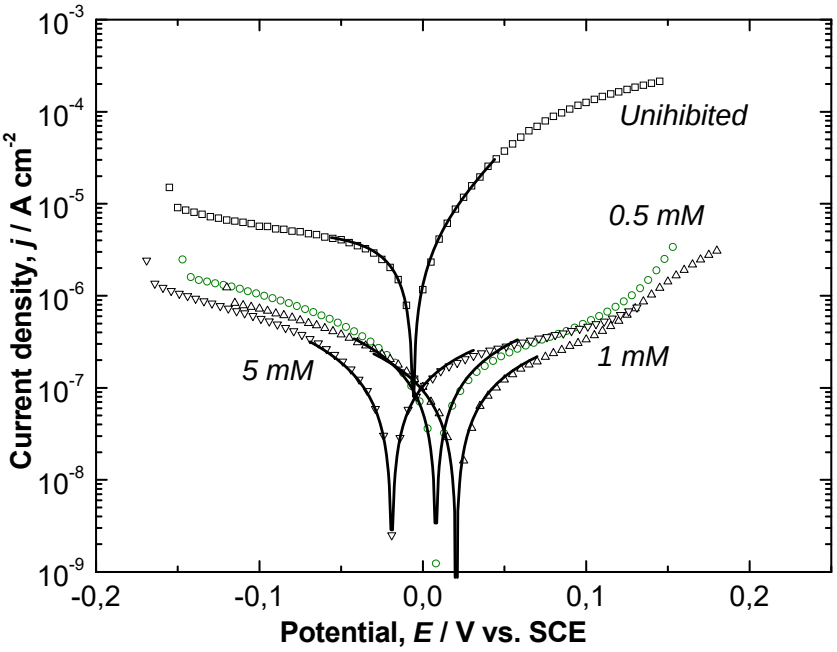

Figure 5. Wide range polarization curves of the Cu-6Sn bronze electrode in Na_2SO_4 / $NaHCO_3$ at pH 5 with different BZI concentrations.

Table 4. Corrosion parameters of in Na_2SO_4 / $NaHCO_3$ at pH 5 with different BZI concentrations, determined by the Tafel extrapolation method.

c, mmol·dm^{-3}	/	**0.001**	**0.005**	**0.01**	**0.05**	**0.1**	**0.5**	**1**	**5**
E_{corr}, mV	-6.40	-31.0	-28.9	-6.03	26.7	-13.0	8.14	20.8	-18.3
b_a, mV·dec^{-1}	54.1	40.4	36.2	38.2	53.7	66.6	121	111	339
- b_c, mV·dec^{-1}	736	362	350	163	177	172	98.4	263	282
j_{corr}, μA·cm^{-2}	4.01	2.39	1.60	0.590	0.301	0.330	0.511	0.402	0.451
z, %	/	40.4	60.1	85.3	92.5	91.8	87.3	90.0	88.8

The corrosion current density presented in Table 4 decreases markedly in presence of the corrosion inhibitor even at very low concentrations, and is the smallest at the concentrations between 0.05 to 1 mmol·dm^{-3}. Further addition of inhibitor does not deteriorate the inhibitive efficiency contrary to other cases examined in this work. The inhibitive efficiency reaches 93 %.

Fig. 6 shows results obtained by the polarization of the bronze electrode in a narrow potential range which indicates that in presence of the inhibitor the polarization resistance increases.

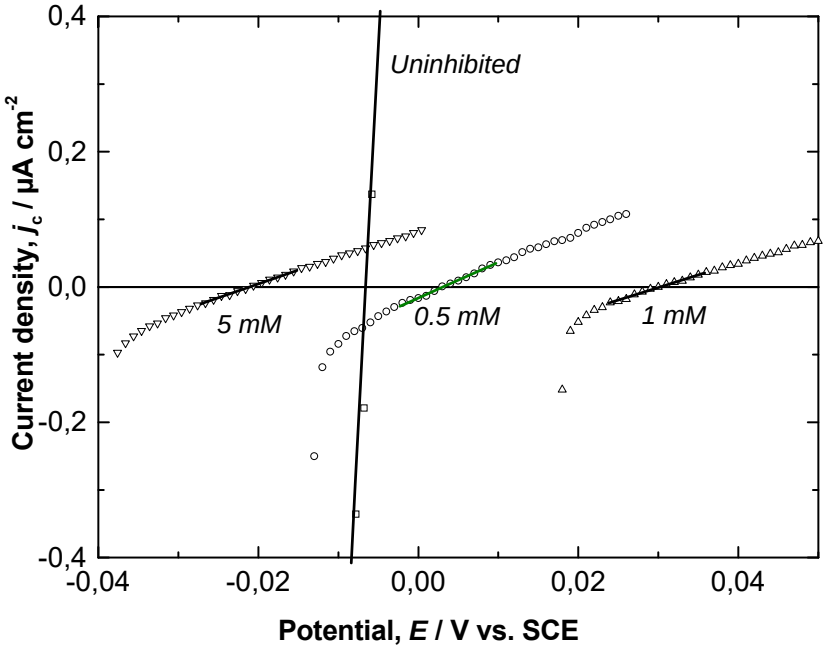

Figure 6. Narrow range polarization curves of bare bronze in Na_2SO_4 / $NaHCO_3$ at pH 5 with different BZI concentrations.

Corrosion parameters of the bronze electrode obtained from these polarization curves are displayed in Table 5.

Table 5. Corrosion parameters of bare bronze in Na_2SO_4 / $NaHCO_3$ at pH 5 with different BZI concentrations, determined by polarization resistance method.

c, mmol·dm^{-3}	/	**0.001**	**0.005**	**0.01**	**0.05**	**0.1**	**0.5**	**1**	**5**
E_{corr}, mV	-7.00	-28.1	-27.3	-18.1	12.9	-10.1	2.99	1.10	-21.3
B, mV	21.9	15.6	14.3	12.6	17.2	20.3	25.7	16.5	48.5
R_p, kΩ·cm^2	4.50	5.21	6.20	21.0	28.6	67.5	197.2	165.0	243
j_{corr}, A·cm^{-2}	4.87	3.00	2.28	0.600	0.600	0.321	0.135	0.331	0.321
z, %	/	38.4	52.8	87.7	87.7	93.4	97.2	93.2	93.4

It can be seen that the value of polarization resistance increases in presence of inhibitor above 0.01 mmol·dm^{-3}, at which the inhibitive efficiency reaches ca. 87 %. It is important to emphasize that BZI decreases the corrosion current density at the concentration as low as 1 µmol·dm^{-3}. The concentration 0.1 mmol·dm^{-3} is sufficient to obtain marked inhibitive effect.

3.2. Patinated bronze

The morphology and the structure of the patinated Cu-6Sn bronze were analyzed by SEM and EDS. Fig. 7 shows the SEM image of the patina.

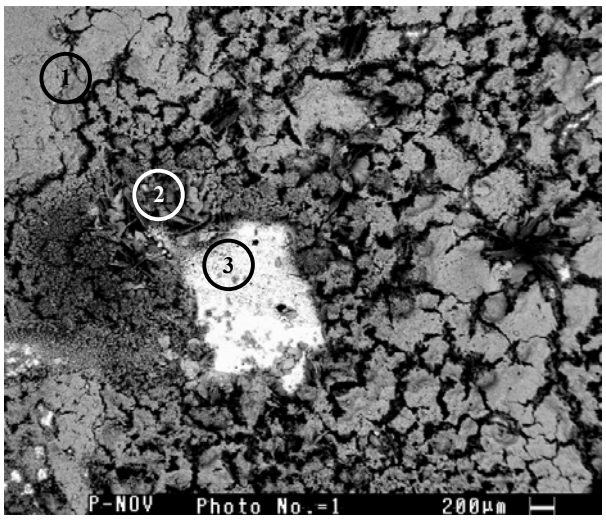

Figure 7. SEM image of the patinated Cu-6Sn bronze.

Three layers can be distinguished on the Cu-6Sn bronze patina (Fig. 7, Points 1, 2, and 3). EDS analyses were also carried out on these layers of the Cu-6Sn bronze patina and they are summarized in Table 6 and represented on the EDS spectra on Fig. 8.

Table 6. The elemental composition (wt-%) of Cu-6Sn bronze patina at the three different positions.

	1	**2**	**3**
Cu	48.3	65.1	79.4
S	0.6	1.0	0.1
O	48.8	29.9	19.0
Sn	0	0	1.4

Layer 1 on the Cu-6Sn bronze (Point 1, Fig. 7) contains a significant amount of oxygen (49 %) and a small amount of sulphur (0.5 %). This means that this layer is formed of copper-oxide, as well as of copper-sulphate.

The crystaline structure that can be observed on the SEM picture as layer 2 (Point 2, Fig. 7) contains a greater amount of copper (65 %) and sulphur (1. %) than layer 1, so it can be assumed that in this part of the bronze copper-sulphate crystals dominate (Fig. 7 and Fig. 8).

Layer 3 (Point 3, Fig. 3) contains mostly copper (79 %) and oxygen (20 %) which form copper-oxyde (Cu_2O) (Fig. 8).

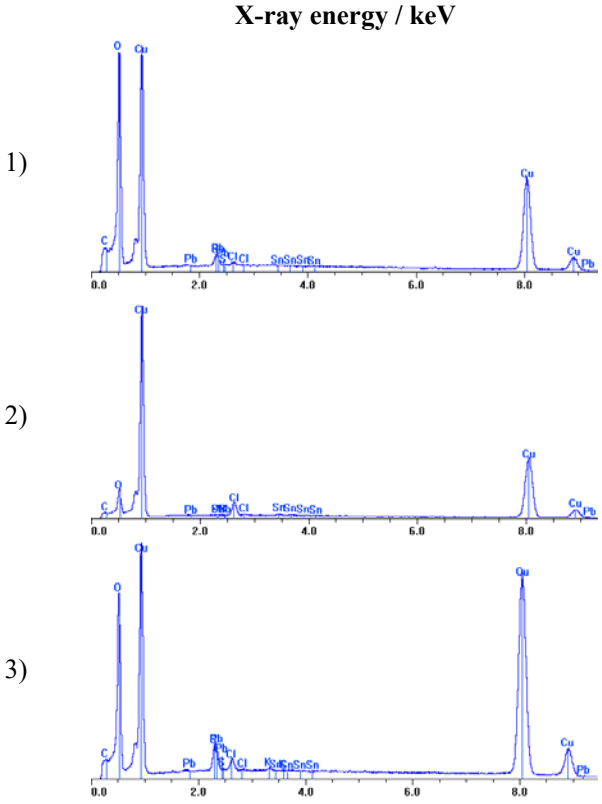

Figure 8. EDS analyses of the Cu-6Sn bronze patina, sampled at the points 1, 2, and 3 marked on Fig. 7.

In all three points on carbon was detected (Fig. 8), but it was unable to quantify it. Thus, it can be concluded that an amount of copper-carbonate was formed on the surface.

Both investigated inhibitors, TMI and BZI, showed a good effect on the corrosion properties of bronze, so they were both tested on bronze covered with patina. Since the Tafel extrapolation method, as well as the polarization resistance method modify the surface state of bronze, or in this case the patina on bronze, impedance spectroscopy was applied in the investigations on patinated bronze. The measurements were performed in each case the same way. An EIS spectrum was recorded prior to inhibitor application: the patinated bronze electrode was dipped into the sulphate / carbonate solution and after a one hour stabilization period an impedance spectrum named “Uninhibited” was collected. The sample was dipped out and dried in air, then dipped again in the corrosion test solution containing the investigated inhibitor. An impedance spectrum was collected after 24 hours.

3.2.1. 4-methy1-1-*p*-tolylimidazole (TMI)

Fig. 7 shows the electrochemical impedance spectra obtained in the solution containing 5 mM TMI. It can be seen from the curves that in presence of TMI the impedance loop is much greater. This shows that TMI protects not only the supstrate bronze, but also the patina when present on bronze and confirms that TMI is a corrosion inhibitor that can be applied on sculptures and other works of art made of bronze.

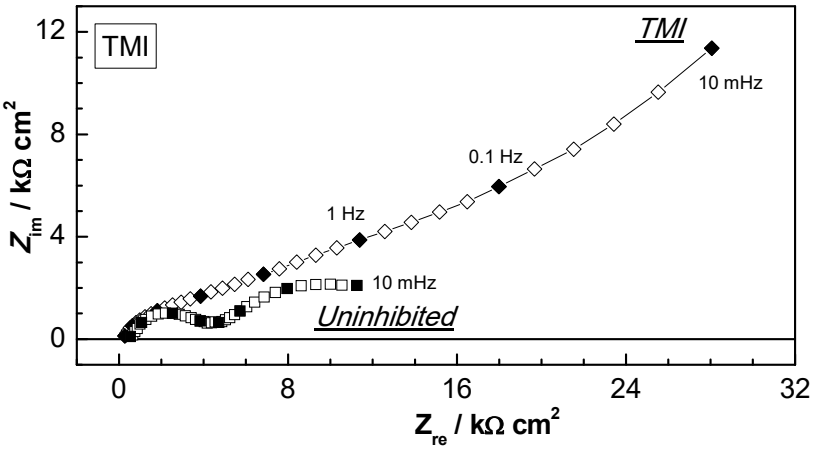

Figure 9. Electrochemical impedance spectra obtained on the electrochemical patina: a) in blank solution and b) prior to experiments in uninhibited solution (Uninhibited) and in the solution containing TMI.

3.2.2. 1-*H* benzimidazole (BZI)

The inhibiting effect of 5 mM BZI with immersion time on the EIS spectra of the electrochemically patinated Cu-6Sn bronze, in the corrosion test solution is presented on Fig. 10.

It can be seen that in presence of BZI, the size of the impedance is much bigger than in the case where it is not present. The difference is much greater than observed in the case of TMI. Both inhibitors showed a protective effect, but BZI showed much better protective properties and as the results on bare bronze have shown a much smaller amount is needed to obtain great results.

4. CONCLUSION

The artificial patina was formed electrochemically on Cu-6Sn bronze under potential regulation in aerated sulphate/carbonate solution which simulates the formation of patina in urban atmosphere.

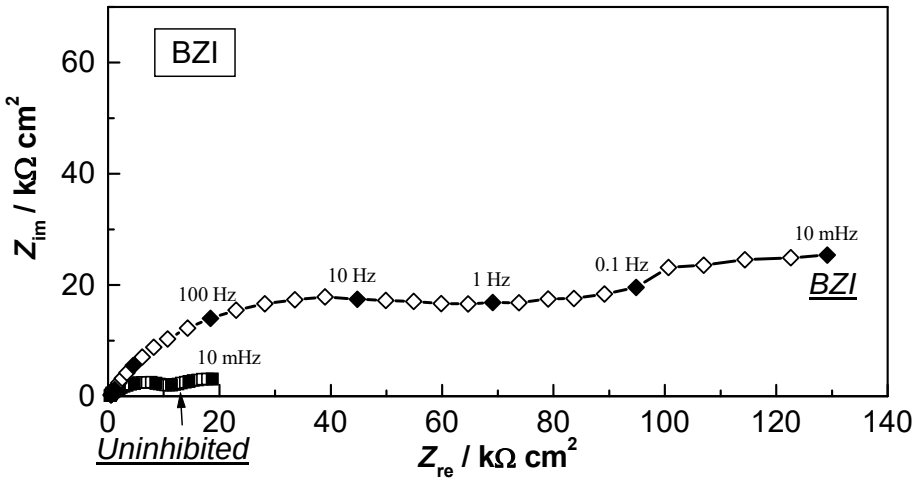

Figure 10. Electrochemical impedance spectra obtained on the bronze covered by electrochemical patina: prior to experiments in uninhibited solution (Uninhibited) and in the solution containing BZI.

The results obtained by SEM and EDS analyses have shown that patina consists of three layers of different textures. Layer 1 is formed of copper-oxyde and copper-sulphate. Layer 2 consists of copper-sulphate crystals. Layer 3 consists of copper-oxyde.

The protective efficiency of two non-toxic imidazole derivatives 4-methyl-1-*p*-tolylimidazole (TMI) and 1-*H* benzimidazole (BZI) was investigated by electrochemical methods on bronze and its patina. The results of the investigations have shown that both organic compounds have protective properties on both bare bronze as well as on its patina in polluted urban atmosphere.

REFERENCES

[1] Rosales, B.; Vera, R.; Moriena, G. Corrosion Science, 1999, 41, 625-651

[2] Rahmouni, K.; Joiret, S.; Robiola, L.; Srhiri, A.; Takenouti, H. Vivier, V. Bulgarian Chemical Community, 2005, 37**,** 26-34

[3] Fuente, D.; Simancas, J.; Morcillo, M. Corrosion Science, 2008, 50, 268-273

[4] Fitzgerald, D. P.; Nairn, J.; Atrens, A. Corrosion Science, 1998, 40, 2029-2050

[5] Fuente, D.; Simancas, J.; Morcillo, M. Corrosion Science, 2008, 50, 268-273

[6] Cicileo, G. P.; Crespo, M. A.; Rosales, B. M. Corrosion Science, 2004, 46, 929-953

[7] Graedel, T. E.; Nassau, K.; Franey, J. P. Corrosion Science, 1987, 27, 639-657

[8] Franey, J. P.; Davis, M.E. Corrosion Science, 1987, 27, 659-668

[9] Nassau, K.; Gallager, P.K.; Miller, A.E.; Graedel, T.E. Corrosion Science, 1987, 27, 669-684

[10] Opila, R. L. Corrosion Science, 1987, 27, 685-694

[11] Muller, J.; Crory-Joy, C. Corrosion Science, 1987, 27/7, 695-701

[12] Graedel, T.E. Corrosion Science, 1987, 27/7, 721-740

[13] Nassau, K.; Miller, A. E. ; Graedel, T. E. Corrosion Science, 1987, 27/7, 703-719

[14] Strandberg, H. Atmospheric Environment, 1998, 32, 3511-3520

[15] Robbiola, L. ; Blengino, J.-M.; Fiaud, C. Corrosion Science, 1998, 40, 2083-2111

[16] Hughes, R.; Rowe, M. The colouring bronzing and patination of metals, Thames & Hudson, London (GB), 1991.

[17] Rahmouni, K.; Takenouti, H.; Hajjaji, N.; Srhiri, A.; Robbiola, L. Electrochimica Acta, 2009, 54/22, 5206-5215

[18] Marušić, K.; Otmačić Ćurković, H.; Takenouti, H. ; Mance, A. D.; Stupnišek-Lisac, E., Chemical and Biochemical Engineering Quarterly, 2007, 21/1, 71-76

[19] Marušić, K.; Otmačić-Ćurković, H.; Horvat-Kurbegović, Š.; Takenouti, H.; Stupnišek-Lisac, E. Electrochimica Acta, 2009, 54, 7106-7113

[20] Muresan, L.; Varvara, S.; Stupnišek-Lisac, E.; Otmačić, H.; Marušić, K.; Horvat Kurbegović, Š.; Robbiola, L.; Rahmouni, K.; Takenouti, H. Electrochimica Acta, 2007, 52/27, 7770-7779

[21] Cronyn, J. M. The Elements of Archaeological Conservation, Routledge, London and New York, 1990, 213-230

[22] Baboian, R. NACE Corrosion Engineer's Reference Book, NACE International, Houston, 2002

[23] Nairn, J. D.; Skennerton, S. G.; Atrens, A. *Journal of Material Science*, 2003, 38, 995-1005

[24] Graedel, T.E.; Nassau, K.; Franey, J.P. Corrosion Science, 1987, **27,** 639-657